NASA MEVTV Program Working Group Meeting: Volcanism on Mars

Oahu, Hawaii
June 27-30, 1988

Sponsored by

LUNAR AND PLANETARY INSTITUTE

Hosted by

UNIVERSITY OF HAWAII AT MANOA

Papers Presented to the

NASA MEVTV Program Working Group Meeting: Volcanism on Mars

Oahu, Hawaii

June 27-30, 1988

Sponsored by
Lunar and Planetary Institute

Hosted by
University of Hawaii at Manoa

LPI Contribution No. 660

* * * * * * * *

Preface

Welcome to Hawaii! Contained within are the abstracts that were received in response to our announcement of the working group meeting. As you know, the purpose of the MEVTV program is to further the understanding of volcanism, tectonism, and volatiles on Mars, and to explore the interactions among these processes.

The purpose of this working group meeting is to focus predominantly on volcanism on Mars, prior to considering the more complex issues of interactions between volcanism and tectonism or between volcanism and global or regional volatile evolution. We also hope to identify the topical areas of research that will aid the planetary geology community in understanding volcanism on Mars and its relationship to other physical processes.

We wish you a stimulating and enjoyable stay in Hawaii!

The Working Group Committee

TABLE OF CONTENTS

ERUPTIVE VISCOSITY AND VOLCANO MORPHOLOGY

Seth B. Posin and Ronald Greeley, Department of Geology, Arizona State University, Tempe, AZ 85287

Terrestrial central volcanoes formed predominantly from lava flows have been classified as shields, stratovolcanoes, and domes. Shield volcanoes tend to be large in areal extent, have convex slopes (1^{o} and 10^{o}), and are characterized by their resemblance to inverted hellenic war shields. Stratovolcanoes have concave slopes, whereas domes are smaller and have gentle convex slopes near the vent that increase near the perimeter. In addition to these differences in morphology, several other variations have been observed. The most important is composition: shield volcanoes tend to be basaltic, stratovolcanoes tend to be andesitic, and domes tend to be dacitic. However, important exceptions include Fuji, Pico, Mayon, Izalco, and Fuego which have stratovolcano morphologies but are composed of basaltic lavas. Similarly, Ribkwo is a Kenyan shield volcano composed of trachyte [1] and Suswa and Kilombe are shields composed of phonolite [2]. These exceptions indicate that eruptive conditions, rather than composition, may be the primary factors that determine volcano morphology [3]. The objective of this study is to determine the relationships, if any, between eruptive conditions (viscosity, erupted volume, and effusion rate) and effusive volcano morphology. Moreover, it is the goal of this study to incorporate these relationships into a model to predict the eruptive conditions of extraterrestrial (martian) volcanoes based on their morphology.

The initial viscosity of lava at the vent ("eruptive viscosity") and its role in determining volcano morphology was assessed. Few measurements of eruptive viscosities have been made and those reported are usually derived through a variety of methods ranging from Jeffrey's equations to various model dependent theoretical calculations. Although these reported eruptive viscosities consitute an important data base, the inconsistency in the method of data acquisition necessitated the addition of a second data base of uniformly derived viscosities. This was accomplished by means of a computer program [4] that estimates the effective viscosity of silicate melts as a function of composition, temperature, and crystal content. The temperatures used were eruptive temperatures measured at, or relatively near, the vent. Due to a lack of data regarding magmatic volatiles and crystal content it was assumed that all lavas were anhydrous and supraliquidous. Additionally, for both the reported viscosities (data base 1) and the calculated viscosities (data base 2), only the lowest eruptive viscosity was selected for each volcanic construct.

Results of the analysis (Fig. 1) show the lowest reported viscosities for 13 terrestrial volcanoes plotted versus the average slopes of the constructs. In addition, calculated viscosities for 18 volcanoes (11 of which are common to data base 1) are shown. For both data bases there is a general trend of increasing viscosity with increasing slope. For the 11 volcanoes common to both data bases the calculated viscosities tend to be lower than the reported viscosities by factors of 10-100. The offset may result from the assumption made in data base 2, that all lavas are supraliquidous; this would explain why the offset increases towards viscous domes which are usually comprised of lavas erupted at lower (subliquidous) temperatures. Therefore, although the 2 data bases define an upper and lower viscosity bound for a volcano of any given slope, the reported viscosities (data base 1) probably offer the best approximation.

In order to apply these results to extraterrestrial volcanoes, the slopes of martian volcanoes [5], lunar domes [5], and venusian volcanoes [6] were inserted into the equations for the best fit lines of data bases 1 and 2 (Table 1). If it is assumed that data base 1 offers the best approximation, then the martian volcanoes have eruptive viscosities typical of Hawaiian basalts, whereas lunar and venusian eruptive viscosities are slightly less. However, there are two important assumptions in this analysis that should be taken into consideration; first, that all the volcanoes listed in Table 1 are effusive--which may not be the case for martian patera [7], and second, that the exposed

portions of semi-buried volcanoes such as Tharsis Tholus accurately represent the geometric shape of the entire volcanic construct.

Efforts are currently being made to refine the morphologic information for both martian and terrestrial volcanoes as well as to develop new methods of expressing volcano morphology. Lava volume and eruption rate data have been assimilated for 75-80 terrestrial volcanic constructs in order to evaluate the effects that each of these eruptive conditions may have on terrestrial and extraterrestrial volcano morphologies.

References

[1] Webb, P.K. and Weaver, S.D. (1975) *Bull. Volc.*, v. 39, p. 294-312
[2] Wood, C.A. (1977) *Abst. Planet. Geol. Field Conf. Snake River Plain, Idaho*, p. 34-39
[3] Schuver, H.J. (1982) *Adv. Planet. Geo.*, p. 565-567.
[4] McBirney, A.R. and Murase T. (1984) *Ann. Rev. Earth. Planet. Sci.*, p. 337-357
[5] Pike, R.J. and Clow, G.D. (1981) Dept. of Interior, USGS, Open File report 81-1038 (preliminary report), p. 1-40
[6] Stofan, E.R. et al. (1987) *Lunar Planet. Sci. Abst.*, p. 952-953
[7] Greeley, R. and Spudis, P.D. (1984) *Rev. Geophys. Space Phys.*, v. 19, n.1, p. 13-41

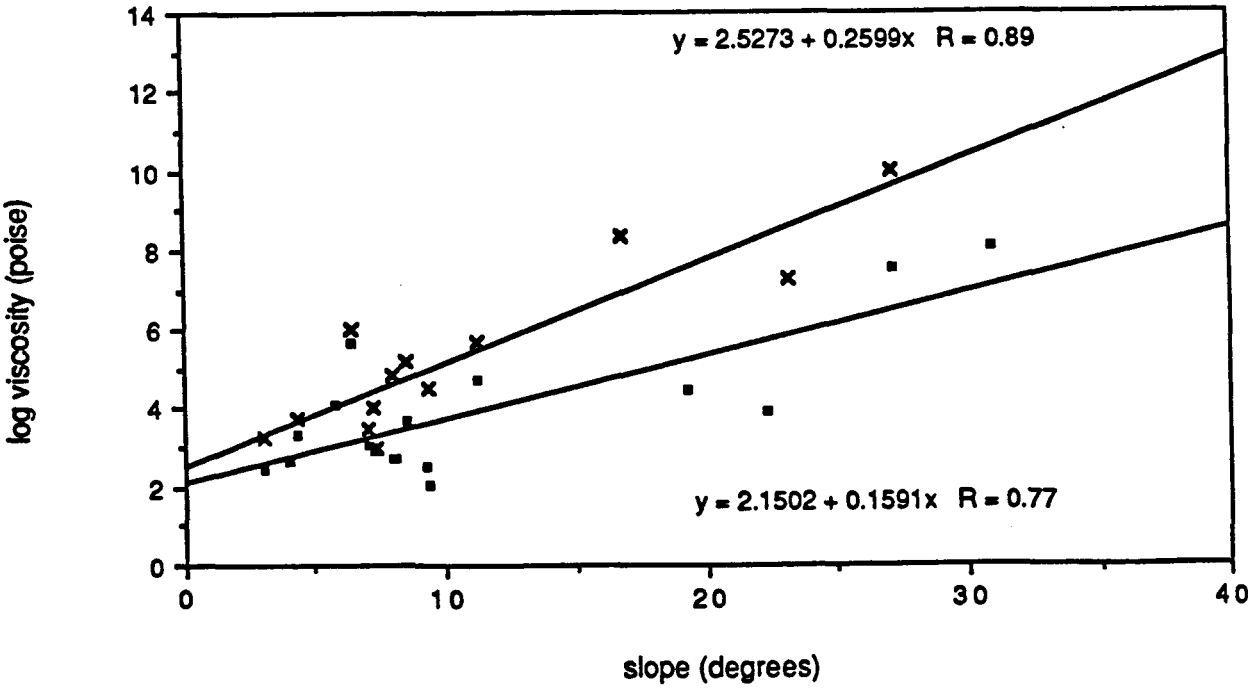

Fig. 1 Plot of log viscosity versus volcano slope for data base 1 (reported viscosities given by ×) and data base 2 (calculated viscosities given by ▪). Equations of best fit line for each data base are shown.

Table 1

Volcano	viscosity (data base 1)	viscosity (data base 2)
(Mars)		
Olympus Mons	3.5×10^3 poise	5.9×10^2 poise
Pavonis Mons	5.8×10^3 poise	7.9×10^2 poise
Ascreaus Mons	1.0×10^4 poise	1.1×10^3 poise
Arsia Mons	1.5×10^3 poise	3.6×10^2 poise
Elysium Mons	2.9×10^3 poise	5.2×10^2 poise
Hecates Tholus	2.0×10^3 poise	4.3×10^2 poise
Uranius Tholus	2.2×10^4 poise	1.9×10^3 poise
Ceraunius Tholus	1.8×10^4 poise	1.6×10^3 poise
Tharsis Tholus	9.3×10^3 poise	1.1×10^3 poise
Albor Tholus	2.3×10^3 poise	4.6×10^2 poise
Jovis Tholus	1.5×10^3 poise	3.5×10^2 poise
Biblis Patera	2.9×10^3 poise	5.2×10^2 poise
Ulysses Patera	3.9×10^3 poise	6.5×10^2 poise
Uranius Patera	7.4×10^2 poise	2.3×10^2 poise
Apollinaris Patera	1.4×10^3 poise	3.4×10^2 poise
(Moon)		
D crater (name prov)	1.0×10^3 poise	2.8×10^2 poise
Maraldi B 2NW	8.1×10^2 poise	2.5×10^2 poise
Cauchy Omega	7.4×10^2 poise	2.3×10^2 poise
Maraldi B 1SE	1.2×10^3 poise	3.1×10^2 poise
Rima Aristarchus 8	9.8×10^2 poise	2.7×10^2 poise
(Venus)		
Theia Mons	8.9×10^2 poise	2.6×10^2 poise
Rhea Mons	1.0×10^3 poise	2.8×10^2 poise

FAULTING AND ITS RELATION TO VOLCANISM: MARS WESTERN EQUATORIAL REGION; David H. Scott and James Dohm, U.S. Geological Survey, 2255 N. Gemini Dr., Flagstaff, AZ 86001.

Recently completed geologic maps of Mars (1-3) show the global distribution of lava flows that were emplaced during each of the three Martian time-stratigraphic periods and the faults and ridges that originated during these periods. These data have been extracted from the geologic maps to make a series of volcano-tectonic maps for the Noachian, Hesperian, and Amazonian Periods. The map series is being compiled on Viking photomosaics at 1:15,000,000 scale. These maps will provide a basis for assessing the interactive roles of volcanism and tectonism in the crustal evolution of Mars.

Volcano-tectonic maps of the western equatorial region of Mars have been completed. Some observations resulting from their study show that volcanic resurfacing in this region has progressively decreased with time from the Noachian Period to the Amazonian. A corresponding decrease in tectonic activity, evidenced by fault densities, occurred mostly during the Amazonian. Exceptions are seen around Alba Patera, where volcanism accompanied by faulting has continued from Hesperian into early Amazonian time and, to a lesser extent, around the Tharsis Montes. The major volcanic centers that include the Tharsis Montes, Alba Patera, Syria Planum and, to some degree, Olympus Mons are the loci of most fault systems. However, many mountains in the western part of the southern highlands that are interpreted to be volcanic (1, 4, 5) lie along arcs that conform to regional trends of fault and ridge systems older than those exemplified by the main tectonic axes of the Tharsis Montes.

Within the western equatorial region, the Tempe Terra volcanic and tectonic province is of particular interest. It consists of three distinct types of terrain (4): rugged hills and mountains, highly faulted ridge-and-valley structures, and relatively smooth uplands extending from the Lunae Planum plateau. Tempe Terra is embayed and partly covered by lava flows from the plains, from Alba Patera, and from the Tharsis Montes. The maps of Figures 1 and 2 (compiled on Viking photomosaics at 1:2,000,000 scale) show the location of faults that originated during the Noachian and Hesperian Periods in the tectonically complex Tempe Terra area. The relative ages of these faults can be deciphered from the stratigraphic position of rock units that either cover them or are transected by them; individual faults or sets of faults can be relatively dated by their degree of degradation and cross-cutting relations.

Results of the studies made at Tempe Terra show four distinct episodes of faulting during the Noachian and Hesperian Periods. Some faulting attributed to the Hesperian Period may have occurred during Amazonian time, but more accurate dating of the faults is prevented by the paucity of Amazonian-age rocks at Tempe Terra. A small volcano (lat 37° N., long 75°) in Tempe Terra, like Alba Patera on a larger scale, has controlled the divergence and concentricity of fault patterns around its center.

REFERENCES

(1) Scott, D.H., and Tanaka, K.L. (1986) U.S. Geol. Survey Misc. Inv. Ser. Map I-1082A. (2) Greeley, Ronald, and Guest, J.H. (in press) U.S. Geol. Survey Misc. Inv. Ser. I-1082B. (3) Tanaka, K.L., and Scott, D.H. (in press) U.S. Geol. Survey Misc. Inv. Ser. Map I-1082C. (4) Scott, D.H. (1982) Jour. Geophys. Res., v. 87, no. B12, p. 9839-9851. (5) Scott, D.H., and Tanaka, K.L. (1981) Proc. Lunar Planet. Sci., no. 12B, p. 1449-1458.

MARS FAULTING AND VOLCANISM

Scott, D.H. and Dohm, J.

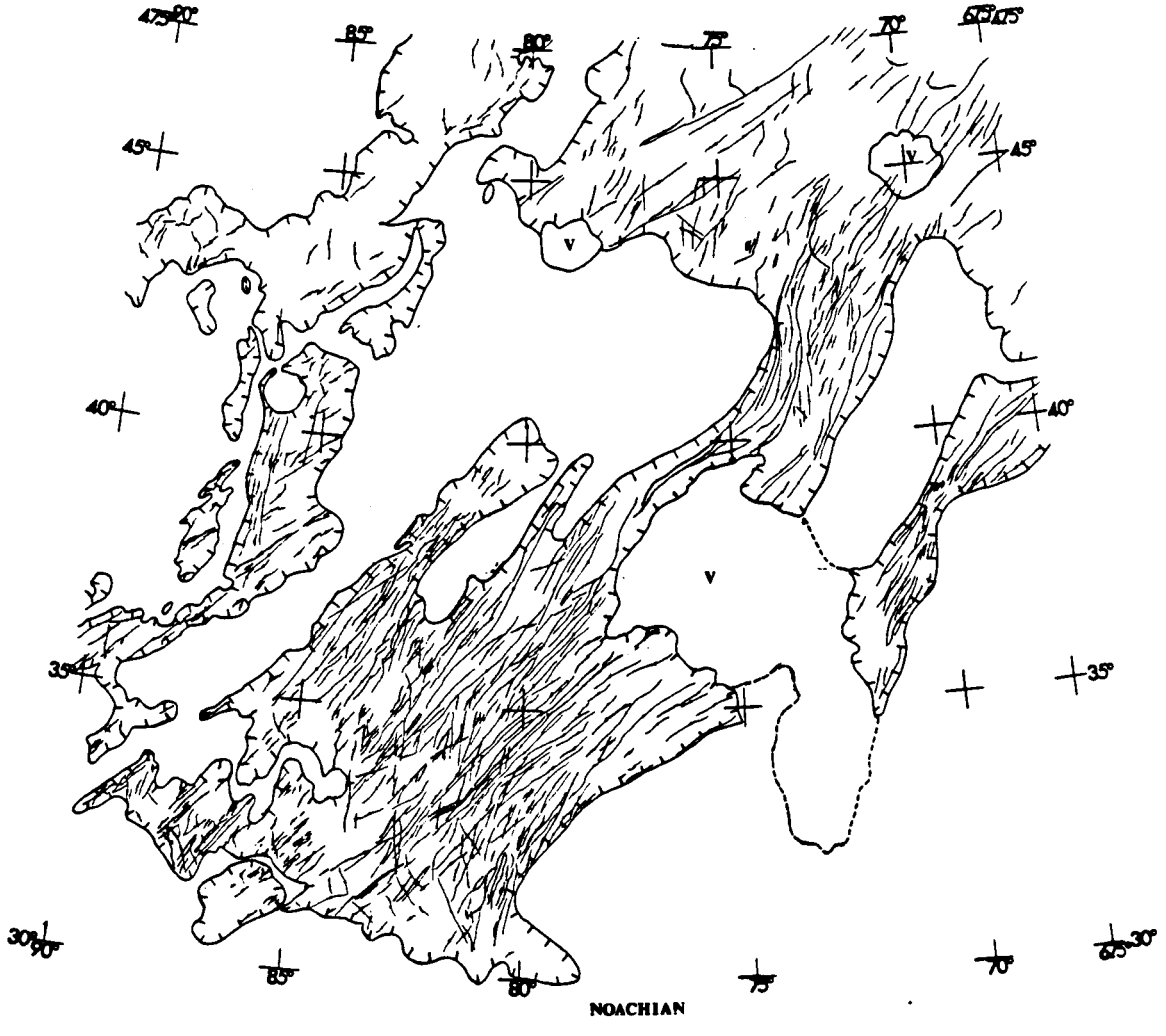

FIG.1

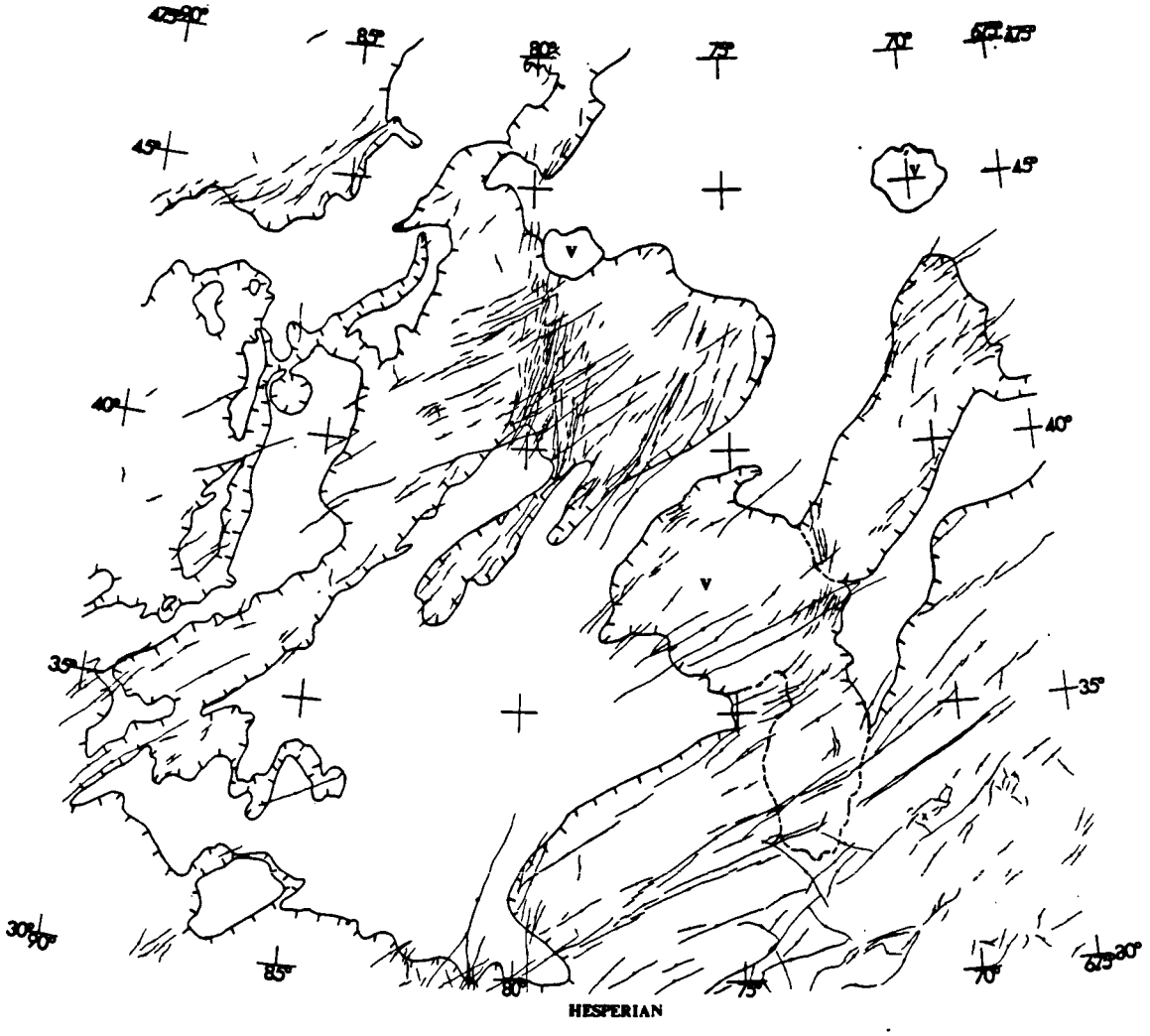

FIG. 2

LAVA THICKNESSES: IMPLICATIONS FOR RHEOLOGICAL AND CRUSTAL DEVELOPMENT. C.R.J. Kilburn (a,b*) and R.M.C. Lopes (c*,d)

(a) Osservatorio Vesuviano, Centro Sorveglianza, Via A. Manzoni 249, 80123 Napoli, Italy; (b*) Dipartimento di Geofisica e Vulcanologia, Università di Napoli, Largo San Marcellino 10, 80138 Napoli, Italy; (c*) University of London Observatory Planetary Image Centre, 33-35 Daws Lane, Mill Hill, London, NW7 4SD, U.K.; (d) Old Royal Observatory, Greenwich, London, SE10 9NF, U.K. (*: Contact Address).

The morphology of a lava flow is strongly influenced by its rheological structure (3,4,5,6,10,11). The rheological structure is, in turn, dependent on numerous factors including: (i) bulk composition, (ii) crystallinity, (iii) vesicularity, (iv) crystal and vesicle size-frequency distributions and, for larger-scale features, (v) crustal development (2). Identifying which of the latter factors are most significant, and hence most readily investigated by remote-sensing techniques, is necessary to clarify short-term objectives and expectations from the study of martian lava flows.

Insights into the rheological controls on flow morphology are provided by variations in thickness of undrained lava streams on Etna and Vesuvius, Southern Italy. Both pahoehoe and aa lavas have been studied. The broken lines in Figure 1 show the limiting trends of the thickness (h)-slope (sin a) relation for Etnean lavas (6), h being measured perpendicularly from the lava surface. The trends are characterised by the relation:

$$h.\sin a = \text{a constant} \qquad \ldots(1)$$

For small slopes and constant density ρ and gravitational acceleration g, $\rho.g.h.\sin a$ is proportional to the basal stress Sb driving lava motion downslope, and so relation (1) becomes:

$$Sb = \text{a constant} \qquad \ldots(2)$$

For a Bingham lava (2,4,6) at equilibrium, Sb = Sy + Sr (5), where Sy and Sr are, respectively, the yield strength of internal lava and the retaining strength of the crust. A simple interpretation of the trends in Figure 1, therefore, is that Etnean lavas come to rest within a restricted range of rheological and crustal conditions.

Thickness-slope data for historical Vesuvian lavas are shown by the filled circles in Figure 1. All the points lie within the Etnean limits, suggesting that lavas on Etna and Vesuvius experience similar rheological and crustal evolutions. Nevertheless, the two suites of lavas have different bulk chemistries and petrographical features: (a) the historical phonolite-tephrites and leucite-tephrites of Vesuvius (7) are potassium-rich and iron-poor compared with the basaltic hawaiites of Etna (2,8); and (b), while the Etnean lavas have similar phenocryst assemblages and typical phenocryst contents of 30-50 vol.% (1,8), four petrographical types have been recognised among historical Vesuvian lavas (12): aphyric, porphyritic with

FIGURE 1

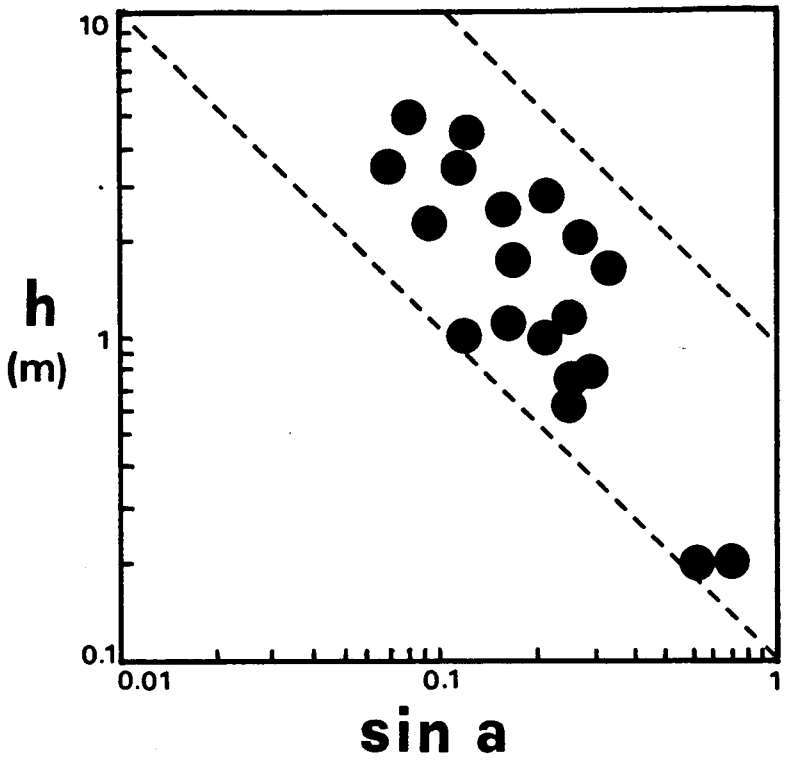

comparable contents of leucite and augite up to 2 mm across, porphyritic with mainly large leucite crystals to 4-5 mm across, and porphyritic with mainly large augite crystals to 5-6 mm long. Vesicle contents and distributions also vary among flows. Hence none of factors (i) to (v) above is clearly indicated for producing the trends in Figure 1.

A common feature of the lavas, however, is their whole-rock silica content which is typically between 47 and 49 wt %. SiO2 is the principal polymerising molecule in common terrestrial magmas and SiO2-content has been proposed as a bulk-rheological index for lavas (4,9). Such a control would be consistent with the trends in Figure 1. Yet it is the deformation of the liquid fraction of a lava, against the resistance of its own molecular structure and of the interaction of contained crystals and vesicles, that characterises its rheological response (2). Hence the inference that whole-rock silica content is closely related to lava rheology and flow morphology may indicate either that:

i. the variation in liquid silica content during crystallisation is negligible compared with the whole-rock silica content; or

ii. groundmass crystallisation (probably during emplacement of the lava) dominates solidification, bringing the ratio {liquid SiO2 content} :

{whole-rock SiO2 content} to a limited range of values, regardless of the earlier sequences of crystallisation represented by the phenocryst assemblages.

Also significant is the fact that an SiO2 control is suggested even though no account has been taken of crustal development. Apparently, therefore, either crusts have not been important in halting the measured flows, or changes in thickness during crustal growth are systematically related to the initial thickness of the uncrusted lava.

REFERENCES:

(1) Archambault, C., and Tanguy, J.C. (1976) J.Volcanol.Geotherm.Res., 1: 113-125.
(2) Chester, D.K., et al. (1985) Mount Etna. The anatomy of a volcano. (Chapman and Hall, London).
(3) Fink, J.H. (1980) Geology, 8: 250-254.
(4) Hulme, G. (1974) Geophys.J.R.Astron.Soc., 39: 361-383.
(5) Kilburn, C.R.J., and Lopes, R.M.C. (1988) J.Geophys.Res. (in press).
(6) Robson, G.R. (1967) Nature, 216: 251-252.
(7) Santacroce, R, ed. (1987) Quad. de "La Ricerca Scientifica" 114, C.N.R. Roma.
(8) Tanguy, J.C., and Clocchiatti, R. (1984) Bull.Volcanol., 47: 879-894.
(9) Wadge, G., and Lopes, R.M.C., manuscript in preparation.
(10) Walker, G.P.L. (1967) Nature, 213: 484-485.
(11) Walker, G.P.L. (1973) Phil.Trans.R.Soc.London, 274A: 107-118.
(12) Washington, H.S. (1924) In: Perret, F.A. (1924) Carnegie Inst. Wash., 339: 1-151.

MARS: VOLCANISM IN THE VALLES MARINERIS OVERLOOKED?; B.K. Lucchitta, U.S. Geological Survey, 2255 N. Gemini Dr., Flagstaff, AZ 86001.

Do volcanic rocks exist in the Valles Marineris? This question is pertinent because the Valles Marineris are gigantic grabens, rivaling rift valleys on Earth in size and depth. They have been interpreted as extensional tectonic structures, perhaps incipient rifts (1, 2, 3, 4). On Earth, rift valleys commonly contain volcanic deposits. On Mars, deposits inside the Valles Marineris grabens do not have the unique morphologic signature of such easily identified volcanic features as shield volcanoes or lava flows. Therefore, many researchers have not recognized the deposits inside the Valles Marineris as volcanic. Is Mars, then, different from Earth in having formed riftlike grabens unaccompanied by volcanism?

An intensive study of high-resolution stereoscopic images found that deposits inside Valles Marineris reflect two episodes of deposition: in the older, a layered sequence was formed that now stands as high eroded mesas approaching the elevation of the bordering plateau (5); in the younger episode, material was deposited on a deeply eroded surface whose elevation is close to that of the present trough floors (6).

The older sequence consists of layers displaying a variety of morphologies and thicknesses. Thin-bedded layers alternate with thick-bedded ones. Some layers are single; others occur in repeated couplets. Dark and light layers are interbedded. Locally, dark layers are more resistant to erosion and form ledges that shed dark talus slopes; light layers tend to be more massive and are dissected by parallel flutes even on low slopes, attesting to susceptibility to wind erosion.

The origin of these deposits is controversial. Volumetric constraints and lack of source areas make it unlikely that the deposits are solely of fluvial or alluvial origin, deposited in water (5, 6). An eolian origin, for instance trapping of wind-blown material in ice-covered lakes (7), is questionable for volumetric reasons also. Therefore, a volcanic origin for the majority of these layered beds is plausible by default more than by incontrovertible evidence. Additionally, as shown below, younger interior deposits are probably volcanic, so that it stands to reason that the older layered deposits also had volcanic components. And, the observed morphologies are consistent with those of volcanic deposits on Earth: dark, resistant layers are similar to terrestrial basalt layers; massive, light layers resemble ash-flow tuffs.

The younger sequence of interior deposits consists of (a) very dark patches that are spectrally relatively blue and have short, stubby lobes in places; they occur characteristically along faults (8); (b) light-colored, thick, smooth deposits that are locally associated with apparent volcanic craters (9); and (c) deposits with lobate fronts, local layering, rough surface textures, and highly irregular albedos. The base of these younger deposits is an unconformity; they embay interior mesas, landslides, and tributary canyons. They are generally thin, but in western Candor Chasma they may reach a thickness of 3,000 meters. These materials are probably volcanic: the dark deposits have spectral signatures similar to mafic rocks on Earth (6); their association with structures suggests internal origin; the locally varied, disordered, and rugged aspect of the thick deposits is not compatible with emplacement by wind; the layering in some sections and lack of a source area make debris-flow origin unlikely; and lobate fronts and embayments suggest flow material.

The very dark patches may be mafic. Because the albedo contrast between the dark and light deposits is not as large as the enhanced images would suggest, the light units could be palagonitic tuffs (10), a composition that also agrees with their reddish spectral signature. On the other hand, young light deposits in places form extensive flat sheets with lobate fronts, perhaps implying ash-flow emplacement; elsewhere, young light deposits are thick and have stubby lobes, implying viscous material. Both of these observations are consistent with volcanism more volatile rich, explosive, and perhaps more felsic than is generally assumed to have occurred elsewhere on Mars.

Overall, results from the study suggest that (a) volcanism was present in the Valles Marineris, (b) the volcanism was explosive in places, (c) some volcanism may have been more felsic than that generally assumed elsewhere, and (d) the younger sequence of interior beds was emplaced so late in Martian history that the planet may be considered to be still volcanically active.

References

[1] Sharp R.P. (1973) Mars troughed terrain. Journal of Geophysical Research, v. 78, p. 4063-4072.

[2] Blasius K.R., Cutts J.A., Guest J.E., and Masursky H. (1977) Geology of the Valles Marineris: First analysis of imaging from the Viking 1 Orbiter primary mission. Journal of Geophysical Research, v. 82, no. 28, p. 4067-4091.

[3] Masson P. (1977) Structure pattern analysis of the Noctis Labyrinthus-Valles Marineris Region of Mars. Icarus, v. 30, p. 49-62.

[4] Wise D.U., Golombek M.P., and McGill G.E. (1979) Tharsis Province of Mars: Geologic sequence, geometry, and a deformation mechanism. Icarus, v. 38, p. 456-472.

[5] McCauley J.F. (1978) Geologic map of the Coprates quadrangle of Mars. U.S. Geological Survey Miscellaneous Investigations Series Map I-897, scale 1:5,000,000.

[6] Lucchitta B.K. (1982) Lakes or playas in Valles Marineris (abs.). Reports of Planetary Geology Program-1982. National Aeronautics and Space Administration Technical Memorandum 85127, p. 233-234.

[7] Nedell S.S., Squyres S.W., and Anderson D.W. (1987) Origin and evolution of the layered deposits in the Valles Marineris. Icarus, v. 70, p. 409-441.

[8] Lucchitta B.K. (1987) Recent mafic volcanism on Mars. Science, v. 235, p. 565-567.

[9] Lucchitta B.K. (1985) Young volcanic deposits in the Valles Marineris, Mars (abs.). Lunar Science 16, The Lunar and Planetary Institute, Houston, Texas, p. 503-504.

[10] Singer R.B. (1982) Spectral evidence for the mineralogy of high-albedo soils and dust on Mars. Journal of Geophysical Research, v. 87, no. B12, p. 10159-10168.

THE MARTIAN HIGHLAND PATERAE: EVIDENCE FOR EXPLOSIVE VOLCANISM ON MARS; ***David A. Crown and Ronald Greeley, Department of Geology, Arizona State University, Tempe, Arizona 85287***

The martian surface exhibits numerous volcanic landforms displaying great diversity in size, age, and morphology [e.g. 1]. Most research regarding martian volcanology has centered around effusive basaltic volcanism, including analyses of individual lava flows, extensive lava plains, and large shield volcanoes. Various eruption mechanisms have been considered theoretically under martian conditions [2,3], and recently a number of investigations have focused on the existence of explosive volcanism on Mars [3-7]. These studies have been hindered by a lack of definitive morphologic criteria for the remote identification of ash deposits. Knowledge of the abundances, ages, and geologic settings of explosive volcanic deposits on Mars is essential to a comprehensive understanding of the evolution of the martian surface, with implications for the evolution of the lithosphere and atmosphere as well as the histories of specific volcanic centers and provinces.

The presence of small-scale or localized explosive volcanic activity is suggested by a variety of features. Cinder cones [8,9] and "pseudo craters" resembling those in Iceland [10] have been identified in the northern plains and in the Tharsis and Elysium provinces on Mars. A smooth, mantled region on Hecates Tholus has been attributed to an airfall deposit resulting from a plinian eruption [3], and volcanic density currents have been proposed to account for channels associated with volcanoes in the Tharsis and Elysium regions [11]. A geomorphic comparison of the Elysium province on Mars with the Tibesti region on Earth reveals similarities between Elysium Mons and terrestrial composite volcanoes [12].

The existence of large-scale explosive volcanic deposits on Mars is controversial. Although the basal scarp [13] and aureole deposits [14] of Olympus Mons and extensive deposits in the Amazonis, Memnonia, and Aeolis regions have been attributed to pyroclastic origins, other hypotheses are implied by the observed morphologies [15-16]. Recently, morphologic evidence has been employed to suggest that pyroclastic deposits are associated with Alba Patera and most likely were emplaced as pyroclastic flows fed by ash fountain eruptions [4,5].

The martian highland paterae (Apollinaris Patera, Amphitrites Patera, Hadriaca Patera, and Tyrrhena Patera) are areally extensive, low-relief features with central caldera complexes and radial channels separating plateau-like erosional remnants [1,17]. The highland paterae, which formed in Upper Noachian to Lower Hesperian time, were intially proposed to be the consequence of eruptions of extremely fluid lavas [18]; however, currently they are believed to be composed predominantly of ash deposits on the basis of morphologic similarities to terrestrial ash sheets [19] and their apparently easily erodible nature [1]. Greeley and Spudis [1], from an analysis of Tyrrhena Patera, proposed an evolutionary sequence for the paterae beginning with extensive pyroclastic eruptions due to the contact of rising magma with the water- or ice-saturated megaregolith followed by erosion of the ash deposits and late stage effusive eruptions with deposits concentrated near the summit.

Hydromagmatic origins for Hadriaca Patera and Tyrrhena Patera have been evaluated quantitatively [6]. Hadriaca Patera is a large, asymmetric volcano with channeled flanks and a central caldera complex filled with smooth plains displaying wrinkle ridges (Figure 1) [20]. Tyrrhena Patera is irregular in plan view and is composed of a lower shield unit of dissected material and a smooth, upper undissected unit containing wrinkle ridges (Figure 2) [1]. Also associated with the late stage summit activity at Tyrrhena Patera are several sinuous rille-like features. The volumes of Hadriaca Patera and Tyrrhena Patera have been estimated from the mapped boundaries of the volcanoes and topographic data from the *1:15M Topographic Map of Mars Eastern Region*. Assuming a density of 1500 kg/m^3 in the deposits, masses for the two volcanoes can be calculated and used to estimate the initial thermal energy of the magmas (Table 1).

If it is assumed that the eruptions producing Hadriaca Patera and Tyrrhena Patera occurred near the present summit regions (and there is no evidence to the contrary), the dimensions of the volcanoes can be used to constrain possible eruption mechanisms. As is the case for Alba Patera, an air-fall origin for most of the deposits can be dismissed because eruption clouds with heights comparable to the total widths of the volcanoes are required [5]. Models for the emplacement of a

gravity-driven flow resisted by a frictional force are used to determine the lengths of terrestrial pyroclastic flows for a given pre-flow topography [21]. The relationship between the flow length and the initial velocity of pyroclastic flows potentially associated with Hadriaca Patera and Tyrrhena Patera for a slope of 0.25° (comparable to the present surfaces of the volcanoes) and for values of the apparent coefficient of sliding friction, μ, equal to 0.05 and 0.10 are shown in Figure 3. Large volume terrestrial pyroclastic flows have values of $\mu = 0.06 - 0.20$ [22]. On Mars, comparable coefficients of friction should be less due to the lower gravity and less dense atmosphere. Figure 3 illustrates that the entire range of paterae flank widths can be produced for both values of μ if only slightly greater than 10% of the initial thermal energy of the magma is converted into the kinetic energy of the pyroclastic flows. This is in agreement with experimental results which indicate a 1 - 10 % energy conversion in hydromagmatic eruptions [23].

Terrestrial magmatic eruptions feed pyroclastic flows either by ash fountaining or by eruption column collapse. To produce flows with lengths comparable to the entire range of flank widths of the paterae, a minimum initial velocity of ~350 m/sec is necessary (for $\mu = 0.05$) (Figure 3). For an eruption driven by magmatic water, this implies an exsolved magma volatile content of > 1%, a mass eruption rate of $>10^7$ kg/sec, and eruption cloud height of nearly 70 km [Fig. 8 in 3]. The eruption rate and column height indicated are similar to those derived for the eruption at Hecates Tholus thought to have produced the mantling deposit seen near the summit.

From an energy perspective origins of Hadriaca Patera and Tyrrhena Patera can be explained by the emplacement of pyroclastic flows fed by eruptions driven by either magmatic or external water. Hydrovolcanic explosions would be favored in the near-surface environment on Mars as water in the megaregolith could come into contact with a rising magma body. Although the magmatic and hydromagmatic models both merit further attention, the formation of the paterae by hydromagmatic eruptions in only an early period of martian history is consistent with suggested global changes on Mars and could explain why this style of volcanism is not evident in later eras.

Table 1. Characteristics of Hadriaca Patera and Tyrrhena Patera

Volcano	Dimensions (km)	Edifice Height (km)	Flank Slopes	Caldera Diameter (km)	Volume (m^3) x 10^{14}	Mass# (kg) x 10^{17}	Thermal* Energy (kg m^2/sec^2) x 10^{23}
Hadriaca	288 x 570	~3	0.05 - 0.60°	63 x 78	1.867	2.801	3.361
Tyrrhena	426 x 660	2+	0.16 - 0.28°	45	1.176	1.764	2.117

#assumes $\rho = 1500$ kg/m^3 in deposits *1 kg $m^2/sec^2 = 10^7$ ergs

References
[1] Greeley, R., and Spudis, P.D., 1981, *Rev. Geophys. Space Phys., 19*, 13-41. [2] Wilson, L., and Head, J.W., 1983, *Nature, 302*, 663-669. [3] Mouginis-Mark, P.J.,Wilson, L., and Head, J.W., 1982, *J. Geophys. Res., 87*, 9890-9904. [4] Wilson, L., and Mouginis-Mark, P.J., 1987, sub. to *Nature*. [5] Mouginis-Mark, P.J., Wilson, L., and Zimbelman, J.R., 1987, sub. to *Bull. Volcanol.* [6] Crown, D.A., Greeley, R., and Sheridan, M.F., *Lunar Planet. Sci. Conf., XIX*, 229-230. [7] Scott, D.H., and Tanaka, K., 1982, *J. Geophys. Res., 87*, 1179-1190. [8] West, M., 1974, *Icarus, 21*, 1-11. [9] Mouginis-Mark, P.J., 1981, *Proc. Lunar Planet. Sci. Conf., 12th*, 1431-1447. [10] Frey, H., and Jarosewich, M., 1982, *J. Geophys. Res., 87*, 9867-9879. [11] Reimers, C.E., and Komar, P.D., 1979, *Icarus, 39*, 88-100. [12] Malin, M.C., 1977, *Geol. Soc. Am. Bull., 88*, 908-919. [13] King, J.S., and Riehle, J.R., 1974, *Icarus, 23*, 300-317. [14] Morris, E.C., 1980, *NASA TM-82385*, 252-254. [15] Schultz, P.H., and Lutz-Garihan, A.B., 1981, *Lunar Planet. Sci. Conf., XII*, 946-948. [16] Tanaka, K.L., 1985, *Icarus, 62*, 191-206. [17] Plescia, J.B., and Saunders, R.S., 1979, *Proc. Lunar Planet. Sci. Conf., 10th*, 2841-2859. [18] Potter, D., 1976, *U.S. Geol. Survey Misc. Geol. Inv. Map I-941*. [19] Pike, R.J., 1978, *Proc. Lunar Planet. Sci. Conf., 9th*, 3239-3273. [20] Albin, E.F., 1986, Master's Thesis, Arizona State University. [21] Malin, M.C., and Sheridan, M.F., 1982, *Science, 217*, 637-640. [22] Sheridan, M.F., 1979, *Geol. Soc. Am. Sp. Paper 180*, 125-136. [23] Wohletz, K.H., 1986, *Bull. Volcanol., 48*, 245-264.

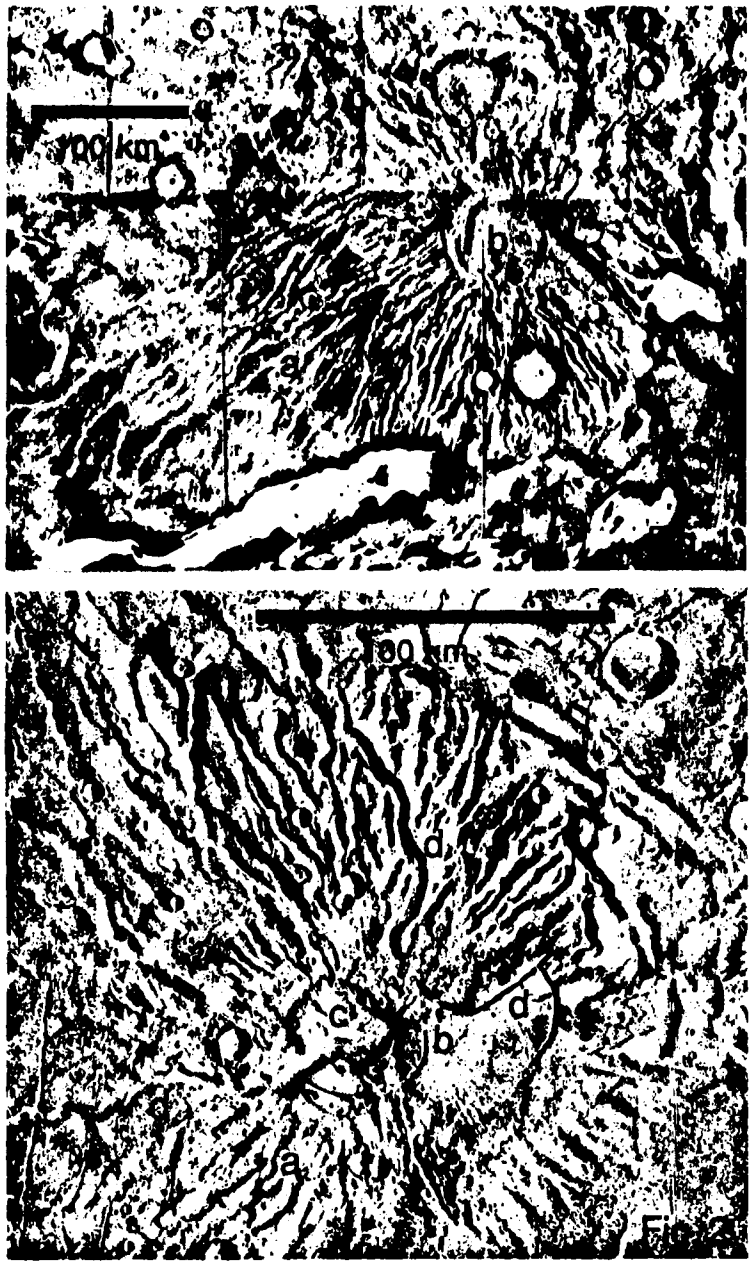

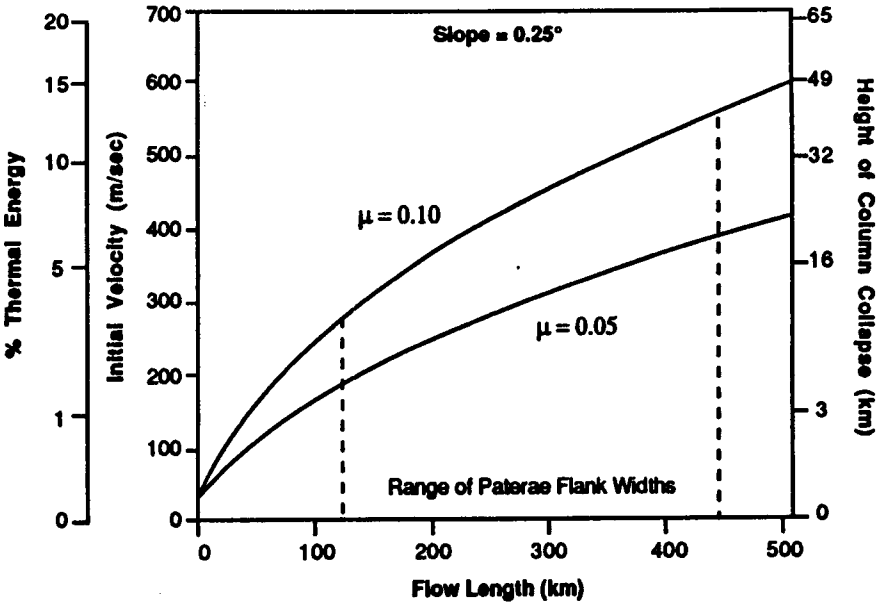

Figure 3.

Figure 1. Viking mosaic of Hadriaca Patera showing (a) dissected flanks and (b) central caldera complex. A large outflow channel and several irregular depressions are evident to the south and west.

Figure 2. Viking image (087A14) of Tyrrhena Patera showing (a) dissected lower shield materials, (b) smooth upper shield materials, (c) central caldera complex, and (d) sinuous rille-like features.

Figure 3. Relationship between flow length and initial velocity for martian pyroclastic flows over a 0.25° slope for coefficients of friction equal to 0.05 and 0.10 [6]. The initial velocity is correlated with the % of the available initial thermal energy of the magma and with a corresponding height of column collapse (by conversion of kinetic energy to potential energy). The observed range of flank widths for Hadriaca Patera and Tyrrhena Patera is indicated.

PHYSICAL PROPERTIES OF SURFACE MATERIALS ON MARTIAN VOLCANOES: DUST-COVERED LAVA AND ASH (?). James R. Zimbelman, Center for Earth and Planetary Studies, National Air and Space Museum, Smithsonian Institution, Washington, D.C. 20560

Remote sensing measurements provide information about the martian surface at scales much smaller than can be inferred from imaging data alone. Measurements of martian volcanoes obtained at visual, infrared and radar wavelengths are discussed here in order to evaluate the physical properties of the volcanic surfaces, in order to assess the contribution of primary volcanic materials to the observed properties. A related issue involves identifying possible ash deposits by distinctive or anomalous physical characteristics.

Visual and near-infrared reflectance. Reflectance values provide information about materials within tens of microns of the surface. Earth-based reflectance measurements can provide considerable spectral resolution (1) but the spatial resolution of these data are insufficient to distinguish individual volcanoes. The Viking orbiter cameras had only limited spectral capabilities but the spatial resolution of images obtained near apoapsis (about 1 km/pixel) is orders of magnitude better than Earth-based measurements (2). The large shield volcanoes in the Tharsis region all display low overall albedos and a large contrast between reflectances at red and violet wavelengths, interpreted to indicate the presence of iron-rich minerals (2). The older Paterae volcanoes in the southern highlands, while not readily distinguishable in the images, also tend to have large red-violet ratios but their albedos are generally similar to that of their surroundings. Unfortunately, the Elysium volcanoes were obscured by atmospheric haze. Monitoring albedo changes on the Tharsis and Elysium volcanoes showed significant seasonal and annual variations on all of the constructs (3), which indicates that the material responsible for the reflectance properties of the volcanoes is mobile. It seems likely that reflectance properties of the volcanoes will be most relevant to the aeolian material deposited and redistributed on the volcanoes.

Thermal infrared emission. The temperature of the martian surface, as obtained from the flux of emitted infrared radiation, provides information about materials within tens of centimeters of the surface. The Viking IRTM experiment provided the first maps of temperature variations on Mars at 30 km spatial resolution, in which the large volcanic constructs in Tharsis and Elysium were shown to have very low thermal inertias (4,5). Thermal inertia can be related to surface particle size through laboratory measurements of thermal conductivity in particulate materials (4,6,7). Thermal inertias obtained from global mapping (4,5) indicate that the Tharsis and Elysium volcanoes have surfaces dominated by fine dust (average size < 50 μm) while the highland volcanoes have surfaces dominated by fine sand (average size about 100 μm). When elevation-dependent effects of the atmosphere are taken into consideration (8), the thermal inertias of the volcanoes

are virtually indistinguishable from that of their surroundings.

Tracks of high spatial resolution thermal measurements (individual spot sizes down to 2 km by 5.5 km) provide additional information about individual volcanoes. Ascraeus Mons has slightly higher thermal inertias on the lower flanks than either at the summit or on the surrounding plains, and all locations measured on the shield have thermal inertias at least an order of magnitude smaller than would be expected for bedrock exposures (9). Similar results are obtained for the other Tharsis Montes and Olympus Mons (10) but thermal inertias tend to increase slightly with increasing geologic age of the shields. Apollinaris Patera, on the boundary between the northern lowlands (low thermal inertia at this location) and the southern highlands (moderate thermal inertia), has thermal inertias higher than those of the Tharsis shields but transitional between values representative of the adjacent regions (11). The trend of increasing thermal inertia with age of the volcanic construct may be related to enhanced consolidation or induration of dust; it seems unlikely that the trend is the result of a change in volcanic style.

Thermal measurements potentially may be affected by the presence of pyroclastic materials at the surface. Graben surrounding Alba Patera have slightly lower thermal inertias than either the Tharsis plains or the central construct, a result difficult to explain by dust retention (12). Geomorphic evidence and theoretical arguments support the possibility that pyroclastic materials comprise a significant portion of the Alba Patera complex and are preferentially exposed around the graben (12). Both moderate and high resolution data indicate the low thermal inertia material surrounding Elysium Mons is centered on a location about 200 km southwest of the volcano (4,13); a study is under way to see if there is geomorphic evidence of pyroclastic activity associated with the unusual thermal inertia distribution (14). Highland paterae (e.g. Tyrrhena Patera) have been proposed to include a significant proportion of pyroclastic material (15) but the thermal data of these volcanoes do not appear to contain signatures distinctive from that of the surrounding highlands.

Radar studies. Reflection or scattering of radar signals provides information about materials within a few meters of the surface. In desiccated materials (as might be expected on Mars) radar signals can penetrate particulates and be reflected, scattered, or absorbed by underlying materials (16). Such penetration seems to be taking place because radar signals from the Tharsis region are very strongly scattered (17-19) by roughness elements that do not affect the low thermal inertia of the region (17). These results indicate that the low thermal inertia material is probably 1-2 meters thick (20).

Topography obtained from Earth-based radar measurements may be useful for selected volcanoes. The Tharsis volcanoes are such strong radar scatterers that signals are not usually returned from them (17,18), except in a depolarized mode (19). The northern flank of Tyrrhena Patera was crossed by two radar

tracks that indicate an average flank slope of < 1° and a total relief that may be < 2 km. Such low slopes support the idea of dominant pyroclastic activity at this volcano. Topographic information may be available for other volcanoes that do not strongly scatter the radar signal.

Flow morphology. Martian flows were emplaced by relatively fluid lava, as evidenced by the great length of some flows, but most flows have calculated yield strengths higher than that of terrestrial basalts (21,22). It is possible that higher yield strength results from increased blockiness (23), which is consistent with enhanced radar roughness for such flows on the Tharsis shields. The increased blockiness could still be masked at visual and thermal wavelengths by a covering of dust.

Summary. 1) Fine dust covers almost everything on Mars, including the volcanoes. 2) The dust on the volcanoes may be slightly compacted or indurated with increasing age of the surface. 3) Dust thickness is usually sufficient to mask the underlying volcanic material at visual and thermal wavelengths but not at radar wavelengths. 4) Pyroclastic materials may influence the thermal properties at a few locations, but the remote sensing signature is not diagnostic; supporting evidence of pyroclastic activity must be obtained from additional sources (e.g. photogeology).

REFERENCES: 1) R.B. Singer et al., J. Geophys. Res. 84, 8415-8426, 1979. 2) L.A. Soderblom et al., Icarus 34, 446-464, 1978. 3) S.W. Lee et al., J. Geophys. Res. 87, 10025-10041, 1982. 4) H.H. Kieffer et al., J. Geophys. Res. 82, 4249-4291, 1977. 5) J.R. Zimbelman and H.H. Kieffer, J. Geophys. Res. 84, 8239-8251, 1979. 6) H.H. Kieffer et al., J. Geophys. Res. 78, 4291-4312, 1973. 7) B.M. Jakosky, Icarus 66, 117-124, 1986. 8) J.R. Zimbelman and R. Greeley, LPS XIV, 879-880, 1983. 9) J.R. Zimbelman, Ph.D. dis., Arizona St. Univ., 1984. 10) J.R. Zimbelman, Trans. Am. Geophys. Union 67, 1074, 1986. 11) D.A. Crown et al., NASA TM-89810, 327-329, 1987. 12) P.J. Mouginis-Mark et al., submitted to Bull. Volc., 1988. 13) J.R. Zimbelman and L.A. Leshin, Proc. LPSC 17th, in J. Geophys. Res. 92, E588-E596, 1987. 14) K. McBride, M.S. thesis work, U. of Houston - Clear Lake, 1988. 15) R. Greeley and P.D. Spudis, Rev. Geophys. Sp. Phys. 19, 13-41, 1981. 16) J.F. McCauley et al., IEEE Trans. Geosci. Remote Sens. GE-24, 624-648, 1986. 17) R.A. Simpson et al., Icarus 36, 153-173, 1978. 18) G.S. Downs et al., J. Geophys. Res. 87, 9747-9754, 1982. 19) J.K. Harmon et al., Icarus 52, 171-187, 1982. 20) P.R. Christensen, J. Geophys. Res. 91, 3534-3546, 1986. 21) H.J. Moore and G.G. Schaber, Proc. LPSC 6th, 101-118, 1975. 22) J.R. Zimbelman, Proc. LPSC 16th, in J. Geophys. Res. 90, D157-D162, 1985. 23) A. Borgia et al., J. Vol. Geoth. Res. 19, 303-329, 1983.

RIFTS OF DEEPLY ERODED HAWAIIAN BASALTIC SHIELDS: A STRUCTURAL ANALOG FOR LARGE MARTIAN VOLCANOES

Michael D. Knight[1], G. P. L. Walker[1], P. J. Mouginis-Mark[1], and Scott K, Rowland[1,2]
[1] Hawaii Institute Geophysics, University of Hawaii, Honolulu, HI 96822
[2] Now at: U.S. Geological Survey, 345 Middlefield Road, Menlo Park, CA 94025

INTRODUCTION: Recently derived morphologic evidence suggests that intrusive events have not only influenced the growth of young shield volcanoes on Mars but also the distribution of volatiles surrounding these volcanoes: in addition to rift zones and flank eruptions on Arsia Mons and Pavonis Mons [1], melt water channels have been identified to the northwest of Hecates Tholus [2], to the south of Hadriaca Patera [3] and to the SE of Olympus Mons [4]. Melt water release could be the surface expression of tectonic deformation of the region or, potentially, intrusive events associated with dike emplacement from each of these volcanoes. In this study we are investigating the structural properties of Hawaiian shield volcanoes where subaerial erosion has removed a sufficient amount of the surface to enable a direct investigation of the internal structure of the volcanoes. Here we report on our field investigation of dike morphology and magma flow characteristics for several volcanoes in Hawaii. We have made a comprehensive investigation of the Koolau dike complex (traceable over 57 km in length by 7 km wide) that passes through the summit caldera. We have also commenced a study of two other dissected Hawaiian volcanoes, namely Waianae and East Molokai. Our goal is not only to understand the emplacement process and magma flow within these terrestrial dikes, but also to explore the possible role that intrusive events may have played in volcano growth and the distribution of melt water release on Mars. We present a compilation of detailed measurements of the associated dike complexes of the major rifts of three deeply dissected relatively old Hawaiian lava-shields, the Koolau (2.6–1.8 Ma) and neighboring Waianae (3.8–2.4 Ma) volcanoes on the island of Oahu, and East Molokai Volcano (1.5–1.3 Ma) on Molokai.

BACKGROUND OF HAWAIIAN VOLCANOES: Active Hawaiian shield volcanoes characteristically have well-defined rift zones within which most of their eruptions are concentrated. Extinct and eroded shield volcanoes charactertistically have dike complexes, these being the subsurface equivalent of the rift zones. Much can be learned about the origin of shield volcanoes by studying the dike complexes. The dike complex of the Koolau volcano is best exposed near sea-level, at about one kilometer erosional depth below the original constructional surface of the shield, making it an ideal location for understanding how the internal plumbing system is related to the overall morphology of a large shield volcano [5]. Koolau dikes are commonly narrower than the basaltic dikes found in other volcanic provinces (e.g. British Isles Province, Decan Traps, Iceland, and the Columbia River Plateau). This narrowness is thought to reflect the generally lower viscosity of Koolau magmas, the closer proximity of the dikes to their volcanic centers or shallow source reservoirs, and the generally lower volume flux of individual eruptive events, particularly when compared to the exceptionally large volume and very thick individual flows (30–100 m) of the great flood basalt provinces.

The Koolau and East Molokai volcanoes (like many of the other Hawaiian lava shields) are commonly composed of nearly equal proportions of both aa and pahoehoe type lavas with few interstratified pyroclastic deposits. The general dip of the lava flows outside the Koolau caldera complex is quite shallow, mostly less than 10° away from either side of the rift axis. In contrast, lavas dip much more steeply (up to 35°–50°) inside the Koolau Caldera and are locally associated with massive caldera collapse breccias composed of lavas and dike rock [5]. Walker suggests that these anomalously high angle basalt flows within the Koolau Caldera are related to centripetal downsagging resulting from many incremental subsidence events.

MEASUREMENTS OF THE KOOLAU DIKE COMPLEX: Measurements of dike strike, dip, size (length, width), magnetic fabric, and fabric morphology indicate that at least two and possibly three magma storage reservoirs could have existed beneath the single volcanic edifice of the Koolau shield. This model for the internal structure of the volcano is based on our measurements of the absolute magma flow direction (inferred from the anistropy and magnetic susceptibility [AMS] magnetic fabric) from 74 dikes [6], the orientation of surface lineations on many other dikes [5], and dike morphology. We suggest that three separate magma bodies were successively emplaced at shallow depths (2–3 km) during the shield building stage (the oldest center was located below the NW-end of Kaneohe Bay, the next oldest center was 12 km to the SE below the S-end of Kaneohe Bay, and the youngest was 8 km further SE below the Koolau Caldera where the Bouguer anomaly reaches its maximum value of +310 mgal. Based on a number of lines of evidence (e.g. dike stratigraphy, field relationships, and magma flow directions) we infer that any two adjacent reservoirs may have been contemporaneously active, feeding the nearly 50 km length of the NW–SE rift system.

The net long-term effect of the many thousands of dike-induced dilations within the dike complex was a significant widening of the Koolau Volcano, but we suspect that the volcano was undergoing synchronous denudation by seaward movement on systems of normal faults and great landslides along the unbuttressed sides of the lava-shield. The best interpretation for the origin of both Koolau and Molokai pali cliff-lines, based on topographic and bathymetric evidence, is given by [7], in which giant submarine landslide-collapse events resulted in catastrophic seaward slumping of major portions (20–30 km wide zone) of the northeastern Koolau and north facing East Molokai shields and exposing the underlying dike complex.

RESULTS: From our analysis of the Hawaiian volcanoes, we find that:

(1) The best model for the formation of the Koolau dike complex is one involving three separate intrusive centers which are thought to be related to multiple shallow (<3 km deep) magma reservoirs within a single volcano. The first of these centers formed near the northwest end of the present shield and the other centers formed southeast of it. We find evidence for a progressive development of centers within a single volcano analogous with the progressive development of volcanoes in the Hawaiian chain. This idea is in agreement with both the plate motion theory over a fixed Hawaiian hotspot and the induced gravitational stresses of a pre-existing Waianea Volcano;

(2) We have made a limited study of the dike complex in the caldera area of the Waianae Volcano, following the recent broad survey by Zbinden and Sinton [8]. Our study of dikes in the Waianae caldera reveals many differences between them and the Koolau dikes. The Waianae dikes have a much more variable chemical composition [8], were intruded at a higher elevation within the edifice, are narrower (48 cm median width), have a more nearly radial distribution, have lower dip angles (commonly <70°), and have steep dilation vectors (direction of opening; commonly plunging >30°); older dikes tend to be more steeply dipping and are often cut by shallow dipping ones. The central Waianae complex presumably formed in a dominantly radial stress field following and/or contemporaneous with the formation of intra-caldera breccias. From the intimate relationship between the dikes, breccias, and brecciated dike rock we infer multiple collapse events, and the complex must have evolved under a low gravitational stress field in isolation from any pre-existing neighboring buttressing edifice;

(3) The wider (67–73 cm), near vertical (85°), low-angle dilational opening (20°), lineated dikes of both the Koolau and East Molokai shields developed in dominantly NW–SE oriented rift systems, apparently each nested against the pre-existing topographic edifice of the Waianae and West Molokai volcanoes, respectively. Hence, these feeder dike

systems evolved in a neutrally buoyant gravitational-induced stress field in which dike propagation was controlled by dike injection parallel to the maximum stress direction;

(4) The general non-vertical nature of the dikes in these Hawaiian complexes, and the non-horizontal orientation of their dilation vectors, implies that injection of the dikes resulted in considerable vertical movement; for every 1 km of horizontal extension in the Koolau complex there was 0.3 km of vertical displacement. The precise significance of this is not fully understood. In the Waianae complex the relative vertical displacement was greater.

(5) Like other Hawaiian shields the rift zones coincide with very high positive Bouguer gravity anomalies that reach a maximum where the calderas are located. These anomalies are thought to represent a much higher proportion of dense intrusive rocks associated with the magma chambers and central conduit system, as well as relatively dense ponded intracaldera lavas. Paradoxically these gravity highs coincide with areas where the intensity of the dike complex drops to a very low value. Walker [5] suggests that the subsidence of the calderas and their environs was very rapid: so rapid was the subsidence that the dike complex has no opportunity of building up to a high intensity. Subsidence and formation of the calderas was possibly by downward creep into a thermally-weakened lithosphere above a hot spot.

IMPLICATIONS FOR MARS: Our study of the Hawaiian dikes leads us to speculate about the following characteristics of intrusive events on Mars:

Multiple magma reservoirs may have existed within a single shield volcano, due to migration of the deep magma source. The most intense distribution of dikes is found to be beneath the assumed caldera center, but dike complexes extend to ~60 km along the rift axis for the Koolau volcano. On Mars, given the regional tectonic control of volcanic provinces such as Tharsis and Elysium [9], we might also expect dike emplacement to extend for tens to hundreds of kilometers away from the volcanic edifices along preferential lines of tectonic weakness.

We also find support for the idea that intrusive events occurred over an extended period of time; intrusions occur during both the growth phase of the volcano and post-caldera collapse. There may therefore be a protracted period of time for a given volcanic center when intrusive events may occur. Thus local areas of melt water release around a given martian volcano (e.g., ref. 2 and 3) could have been associated with changes in the location of the magma reservoir or tectonic structure due to the growth of the volcanic edifice itself.

REFERENCES:

[1] Mouginis-Mark, P. J., S. H. Zisk, and G. S. Downs, Nature, 297, 546–550, 1982.
[2] Mouginis-Mark, P. J., Icarus, 64, 265–284, 1985.
[3] Squyres S. W., D. E. Wilhelms, and A. C. Moosman, Icarus, 70, 385–408, 1987.
[4] Mouginis-Mark, P. J., Recent water release in the Tharsis region of Mars, submitted to Icarus.
[5] Walker, G. P. L., U.S. Geol. Survey Prof. Paper, 1350, 961–993, 1987.
[6] Knight, M. D., and G. P. L. Walker, J. Geophys. Res., 93, 1988.
[7] Moore, J. G., U. S. Geol. Survey Prof. Paper 501-D, 95–98, 1964.
[8] Zbinden, A. E., and J. M. Sinton, The dike swarm of Waianae Volcano, Oahu, submitted J. Geophys. Res.
[9] Solomon, S. C. and J. W. Head, J. Geophys. Res., 87, 9755–9774, 1982.

SIMULATIONS OF LAVA FLOWS ON MARS, S. Baloga and J. Crisp, Jet Propulsion Laboratory, CalTech, Pasadena CA, 91109

One way to approach the understanding of the lava flows observed in the Viking images is to use well-documented terrestrial flows and to simulate comparable eruptions adjusted for martian conditions. The detailed documentation available for several episodes of the 1983-4 PuuOo eruption [1, 2] can be used in combination with an extension of the emplacement theory for solitary lobate flows [3, 4] to simulate comparable eruptions on the surface of Mars. For simplicity, the simulation is restricted to differences in the gravity between Earth and Mars.

The first major issues that need to be addressed for terrestrial flows are how the viscosity of the magma changes with distance from the vent and how well a theoretical description of emplacement agrees with the observed data. Conservation of lava volume at each step along the path of a flow is described by

$$W\,(\partial h/\partial t) + \partial Q/\partial x = 0 , \tag{1}$$

where the flow rate is given by

$$Q = g \sin\theta\, h^3\, W / (3\nu) \tag{2}$$

(see Table 1 for definition of symbols). The overall conservation of volume requires

$$V(t) = \int_0^t Q(0,t')\, dt' = \int_0^L W(x)\, h(x,t)\, dx , \tag{3}$$

These formulations account for (but do not predict) changes that occur in the width of the flow and the pre-existing slope of the flow bed.

If the effusion rate feeding a particular lobe is approximately constant, then the thickness of the flow is given by

$$h(x) = h_o \left[\frac{\nu(x)}{\nu_o} \frac{W_o}{W(x)} \frac{\sin\theta_o}{\sin\theta(x)} \right]^{1/3} , \tag{4}$$

More importantly,

$$\frac{\nu(x)}{\nu_o} = \frac{\sin\theta(x)}{\sin\theta_o} \left[\frac{W_o}{W(x)} \right]^2 \left[\frac{Q_o}{W_o h_o} \frac{dt}{dx} \right]^3 , \tag{5}$$

where t(x) denotes the time when the flow front was a distance x from the vent. To make this theory of emplacement self-consistent we must also have t(x) satisfy

$$\lim_{x \to 0} dt/dx = a , \tag{6}$$

where $a = (h_o/\langle h\rangle)\ (W_o/\langle W\rangle)\ (T/L)$.

Good data for applying this theory is available for many of the episodes of the Puu Oo eruptions. Specifically, we need data on the advance of the flow, the local topographic slope and the total width of the flow. Such data have been used in the theory for three of the Puu Oo episodes to compute the viscosity as a function of distance, measured along the path of the flow. A typical result is shown in Figure 1. Figure 2 shows a linear fit for log viscosity versus time for a combined data set of three Puu Oo episodes. All three data sets exhibit the same general increase in viscosity, approximately one half order of magnitude per day.

Using this relationship between viscosity and time (Fig 2) for the Puu Oo flows, we can return to equation (4) and compute the theoretical flow thicknesses. Figure 3 shows a typical comparison of the predicted flow thicknesses with those measured in the field. The agreement between theoretical and observed flow thicknesses is very reasonable, except at a few points at the final location of the flow front. The results for other episodes are similar. Thus volume conservation and simple viscous flow dynamics appear to provide a satisfactory description of the general features of the emplacement process for solitary lobate flows on Earth.

For a martian flow with the same constant Q, W(x), and $\sin\theta(x)$ as the Puu Oo episode 4 flow, we used the theoretical model to determine how viscosity would increase as a function of distance. In order to scale the problem for the gravity difference between Earth and Mars, equation (2) requires the following changes:

$$h_o \rightarrow 1.39\ h_o\ , \quad t(x) \rightarrow t/1.39\ , \quad \nu(x) \rightarrow \nu(1.39x)\ . \qquad (7)$$

Thus, for a simulated martian flow, the flow front advances more slowly, the flow is thicker near the source, and viscosity increases more rapidly with distance than for corresponding terrestrial flows. The results for the Puu Oo episode 4 flow are shown in Fig.3. For this example, the simulated martian flow reaches 6 km in about 4 days, whereas the Puu Oo flow went 6 km in 2.8 days. These results imply that for comparable flow rates, martian flows should be shorter (or cover less area) than flows on Earth.

TABLE 1. Symbols (Note: subscript "o" is used to denote "at the source")

h	flow thickness	θ	slope of the flow bed
<h>	average flow thickness	V	flow volume
L	flow length	ν	flow viscosity
Q	flow rate	W	flow width
t	time	<w>	average flow width
T	total duration of the flow	x	distance from the source

REFERENCES: (1) Wolfe, E.W., M.O. Garcia, D.B. Jackson, R.Y. Koyanagi, C.A. Neal, and A.T. Okamura (1987) USGS Prof Paper 1350, 471-508 (2) Wolfe, E.W., C.A. Neal, N.G. Banks, and T.J. Duggan (in press) USGS Prof Paper 1463 (3) Baloga, S. (1987) JGR, 92, 9271-9279 (4) Baloga, S. (1986) JGR, 91, 9543-9552

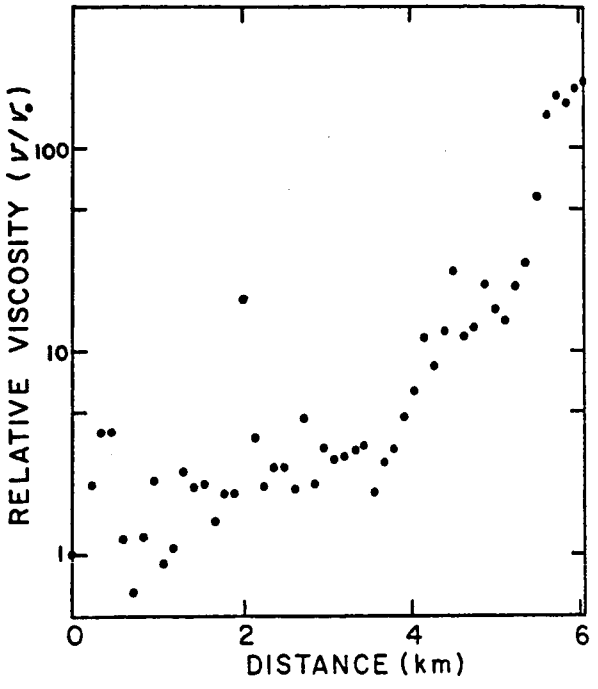

Fig 1: Computed relative viscosity versus distance for Puu Oo episode 4

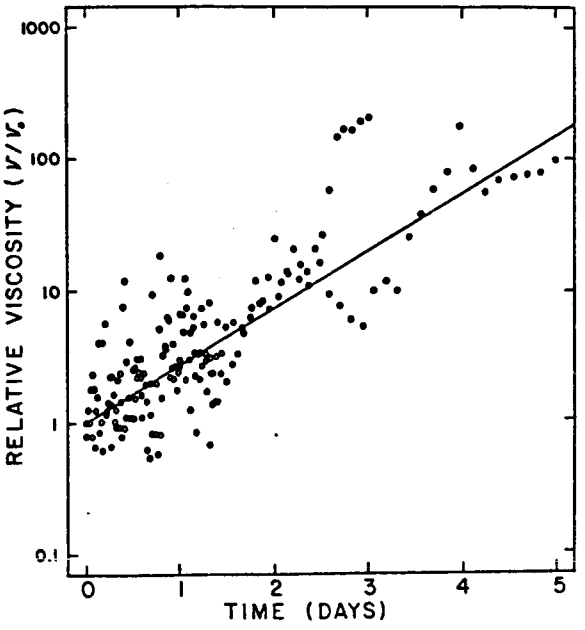

Fig 2: Computed relative viscosity versus time for Puu Oo episodes 2, 4, and 18, with a linear least squares fit fixed at (0,0).

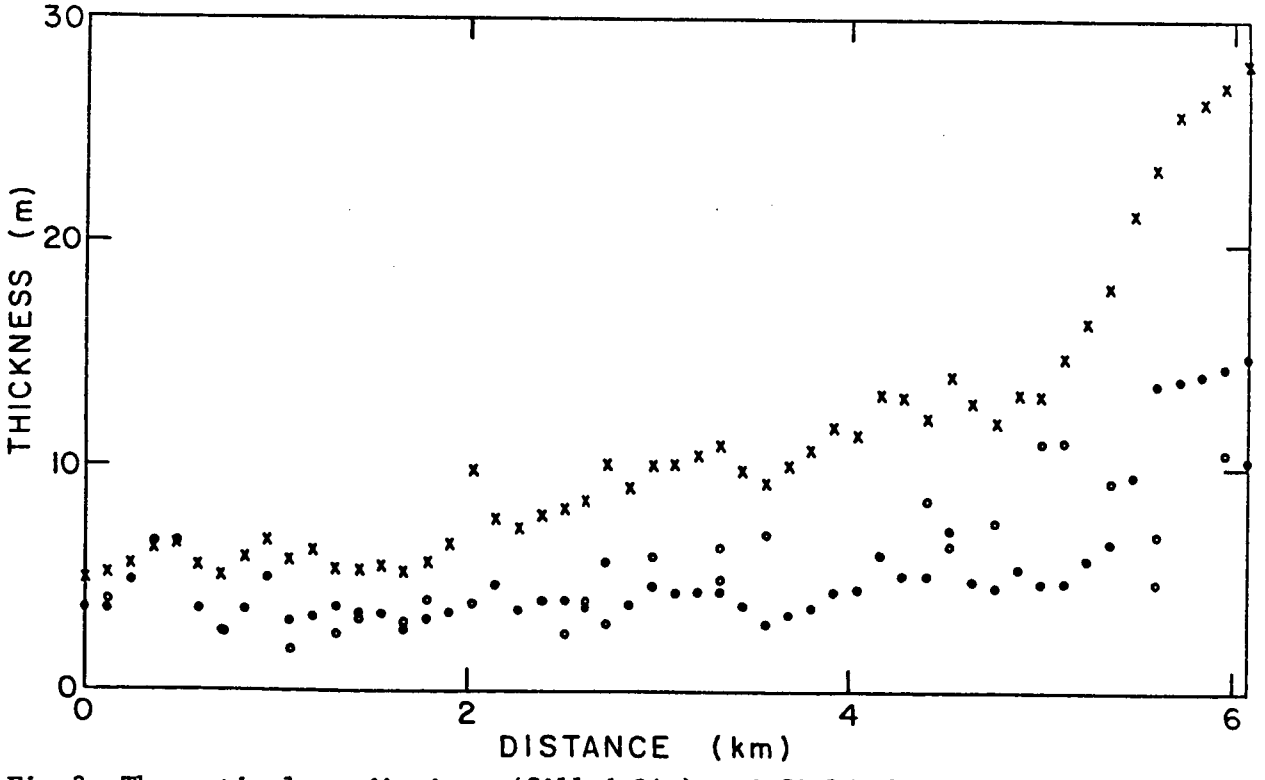

Fig 3: Theoretical predictions (filled O's) and field observations (open O's) of flow thicknesses versus distance for Puu Oo episode 4. Computed thickness of simulated martian flow (X's), as a function of distance.

SMALL-SCALE VOLCANIC LANDFORMS INDICATIVE OF DISTRIBUTARY TUBE SYSTEMS; E. Theilig, National Research Council at Jet Propulsion Laboratory, California Institute of Technology, Pasadena, CA

Surface features tens to hundreds of meters in size on martian lava flows are revealed in high resolution Viking Orbiter images (1,2). Many of these morphological features form in response to certain flow emplacement mechanisms, eruptive styles, or rheological properties of the lava. Insight into the relationships between lava flow morphology and the emplacement and characteristics of magma is an ongoing area of research and allows constraints to be placed on interpretation of martian volcanism. This report focuses on pressure ridges, tumuli, and pressure plateaus which comprise a suite of features characteristic of compound pahoehoe lava flows. Similar ridges and mounds have been identified in the Tharsis region of Mars (2).

Elongate pressure ridges, circular tumuli, and large irregular pressure plateaus are arched or domed shaped and are characterized by open wedge-shaped cracks at their summits. The similar morphology suggests a single formational mechanism for all of these features. Previous studies, primarily based on observations of Hawaiian lava flows, have concentrated on tumuli and have proposed that these features formed by uplift of weak surface crust behind blocked lava tubes (3). Widespread occurrences of pressure ridges and plateaus, however, are predominantly found on sections of lava fields lacking evidence of master tube systems or large channels from which crusted over tubes could have formed. This apparent lack of correlation between large scale tube development and occurrence of pressure ridges and plateaus suggests a different mechanism than that previously proposed for tumuli.

Field observations on the McCartys flow, New Mexico, and the Wapi flow, Idaho (4) and theoretical modeling (5) indicate that pressure ridges and plateaus form as part of the flow process and can be used to interpret the emplacement mechanism (6). Each ridge or plateau occupies the central part of individual flow lobes or toes and, in plan view, mimics the lobe margins. The emplacement process described below only pertains to a single lobe a few to tens of meters wide and occurs contemporaneously in numerous lobes across the lava field. Lava effused from a bocca or series of boccas advances to form a small lobe. Flow advance slows or halts and continued influx of lava causes the lobe to inflate. Upward driving pressure of the lava is resisted by the strength of the crust and the amount of deflection is controlled by applied pressure, dimensions of the area being uplifted, and thickness of the crust. As the surface is deformed upward, cracks form where tensile stress is greatest and open downward over the center of uplift and upward around the edges. Molten lava from the interior fills the cracks and may break out through fractures penetrating the crust. Predominant secondary effusion of lava occurs through boccas at the base, where local hydrostatic pressure is greatest. If lava supply is uninterupted, the process may repeat and another lobe forms.

Several aspects of this emplacement mechanism are consistent with tube-fed flow. For inflation to occur, lava must pond behind a slowly moving front and must be contained by a congealed crust. Columnar joint surfaces forming the upper part of crack walls suggest formation of a 0.2 to 1 m thick crust prior to uplift. Effusion of lava through cracks generated during deformation of the crust provides evidence of molten lava moving through the ridge/plateau interior. The budding lobe and toe mechanism of tube formation (7) probably operated during emplacement of the small lobes. The lobes were emplaced on the surface and inflation occurred along their entire length. As numerous lobes formed by continual repetition of this process, a distributary tube system developed.

Flow rate and topographic slope probably control this style of flow emplacement. Increased viscosity and yield strength caused by cooling of the tube margins eventually results in slowing or halting flow advance. Cooling of the margins to halt a flow suggests a balance, expressed by the dimensionless Graetz number, between cooling rate and flow rate (8-10). Flow rates for lobes containing ridges and plateaus were calculated from a Graetz number analysis and were found to vary between 0.05 and 10 m^3s^{-1}. These rates are on the lower end of measured values for Hawaiian flows (3,11,12). Onset of pressure ridge occurrence within a lava field is typically associated with a break in slope with most ridges restricted to slopes $<1^0$. Low velocities would result from a combination of low flow rate effusion onto gentle slopes.

Flows characterized by pressure ridges and plateaus are different than those emplaced by tubes formed from crusted over channels. Instead of establishing well defined channeled flows, a complex distributary tube system forms across the entire field by budding. On low slopes, the flow advanced slowly through numerous lobes that constructed tubes as they extended. Within individual tubes, cooling of the margins caused the flow to stagnate and inflation occurred along the length of that tube. Uplift then created a ridge or plateau depending on the geometry of the initial tube. In contrast, tumuli may form as point source uplifts, either as a small inflated tube or behind a blocked buried tube. As such, tumuli are not indicative of a specific tube emplacement mechanism. Where pressure ridges and plateaus can be identified on Mars, they can be used to interpret the flow emplacement process.

Most of this work was conducted at Arizona State University.

REFERENCES

(1) Schaber G.G. (1980) Icarus 42, p. 159-184.
(2) Theilig E. and Greeley R. (1986) Proc. Seventeenth Lunar Sci. Conf., J. Geophys. Res. 91, p. E193-E206.
(3) Swanson D.A. (1973) Geol. Soc. Am. Bull. 84, p. 615-626.
(4) Theilig E. and Greeley R. (1987) Geol. Soc. Am. Abstract with Progam 19, p. 866.
(5) Theilig E. and Greeley R. (1985) EOS, Trans. Am. Geophys. Union 66, p. 1125.
(6) Theilig E. and Greeley R. (1988) Accepted for Bull. Volcan.
(7) Peterson D.W. and Swanson D.A. (1974) Stud. Speleology 2, p. 209-222.
(8) Pinkerton H. and Sparks R.S.J. (1976) J. Volcan. Geotherm. Res. 1, p. 167-182.
(9) Hulme G. and Fielder G. (1977) Philos. Trans. R. Soc. London A285, 227-234.
(10) Wilson L. and Head J.W., III (1983) Nature 302, p. 663-669.
(11) Moore R.B., Helz R.T., Dzurisin D., et al. (1980) J. Volcan. Geotherm. Res. 7, p. 189-210.
(12) Wolfe E.W., Garcia M.O., Jackson D.B., et al. (1987) U.S. Geol. Surv. Prof. Paper 1350, p. 471-508.

Volcanic Styles At Alba Patera, Mars: Implications Of Lava Flow Morphology To The Volcanic History; D. M. Schneeberger and D. C. Pieri, Jet Propulsion Laboratory, California Institute Of Technology, Pasadena, California 91109

Alba Patera presents styles of volcanism that are unique to Mars. Its very low profile, large areal extent, unusually long and voluminous lava flows, and circumferential graben make it among Mars' most interesting volcanic features. Clues to Alba's volcanic history are preserved in its morphology and stratigraphy. Understanding the relationship of lava flow morphology to emplacement processes should enable estimates of viscosity, effusion rate, and gross composition to be made (1,2).

Lava flows, with dimensions considered enormous by terrestrial standards, account for a major portion of the exposed surface of Alba Patera (figure 1). These flows exhibit a range of morphologies (3,4,5,6,7). While most previous works have focused on the planimetric characteristics, we draw attention to the important morphological attributes, paying particular attention to what the features suggest about the emplacement process.

The flows at Alba have been divided into two major morphological groupings: tabular flows and crested flows (8). Almost all are radial to the central caldera complex. There appear to be two general styles of tabular flows: solitary and intercalated (figures 1a,1b). The latter tend to occur in intimate association with complex superpositional relationships, giving them a stacked or layered appearance. Similar flows, not nearly as well developed as at Alba Patera, occur north and west of Elysium Mons and Hecates Tholus, respectively. Other flow types identified at Alba include sheet flows, possible leveed (levee-like) flows, undifferentiated flows, and pyroclastic flows. The sheet flows are those with poorly defined flow fronts that appear to be emplaced regionally as might be expected with a flood lava (figure 1c). The levee-like flows typically are small and have a disproportionately wide "levee" as compared to the overall flow dimensions. The undifferentiated flows are those so closely spaced that their individual character cannot clearly be recognized. Ash deposits (pyroclastic flows) have been suggested by Mouginis-Mark et al. (9) as an explanation for the dissected terrain on the northwest flank of the volcano (figure 1d).

Photo-geologic mapping of the Alba Patera indicates that the region can be divided into three major zones. The lowermost consists of areally extensive sheet (presumably flood) lavas and the dissected terrain (pyroclasitc deposits?). Above this, the intermediate zone is made up of tabular flows and crested flows. This zone is split into two sub-zones with the flows in the upper being cut by the circumferential graben. Tabular flows here are both solitary and intercalated, and are large. The uppermost zone is characterized by tabular flows typically smaller than those found in the intermediate zone. Examples of levee-like flows were identified north and west of the caldera margin. Included is an area of undifferentiated flow material. Crested flows are noticably absent from the uppermost zone. Preliminary estimates (10) of the relative sequences for eight selected flows suggest a dichotomy in ages between the intermediate and uppermost zones.

The morphology and superpositional relationships of the flows and other volcanic features suggests that Alba experienced a rather complex formative history. The earliest effusion of lavas appears to have been from the northeast trending graben system radial to Tharsis. The sheet flows that make up the lowermost unit resemble flood lavas apparently unrelated in orientation to the central caldera complex. Following their emplacement, volcanic activity began to localize near the present caldera. During this time what appear to be pyroclastics were erupted from central vents along the flanks of Alba (9). Based on their radial orientation, the remainder of the flows at Alba Patera appear to have been erupted from a centralized source, presumably at or near the present location of the caldera

(figure 1e). The quiet but sustained effusion of what were probably low viscosity lavas began producing crested flows with long and sometimes sinuous axial longitudinal valleys or longitudinally-aligned pits. These flows may have well-developed lava tubes as evidenced by what appears to be collapsed tube structures along apical ridges on the flows (figure 1f). Voluminous tabular flows (11) were also produced during this period. The overall dimensions of individual tabular flows (particularly thickness) are considerably greater at the distal reaches of the flow than for crested flows. We suspect that the tabular flows, in contrast to the crested flows, represent a different style of effusion which may have been characterized by episodic surges of lavas.

Isolated evidence of contemporaneous graben formation is preserved by flows that show signs of being captured and temporarily diverted (figure 1g). If other flows experienced this, then the evidence has been subsequently buried since nearly all of the exposed flows are cut by subsequent graben formation.

The last major effusive activity at Alba was marked by a reduction in the volume of lava being produced. Small solitary tabular flows were emplaced; many coalescing to produce undifferentiated flow material within the circumferential graben system. During this activity, a few levee-like flows were produced. Such an occurrence may indicate an increase in viscosity near the end of Alba's activity. Termination of volcanic activity at Alba was marked by the final collapse of the caldera. Continuation of graben formation after lava effusion is suggested by the many shallow graben near the summit region that cut the flows while showing no sign of being infilled or flooded.

This work was carried out under contract to NASA at the Jet Propulsion Laboratory, California Institute Of Technology, Pasadena, CA.

REFERENCES:

(1) Baloga S. M. and Pieri, D.C., 1986, Jour. Gephys. Res., 91, pp.9543-9552. (2) Pieri, D. C., 1987, NASA TM-89810, pp.354-356. (3) Carr, M. H., et al., 1977, Jour. Geophys. Res., 82, pp.3985-4015. (4) Carr, M. H., and Greeley, Ronald, 1980, NASA SP-403. (5) Carr, M. H., 1981, The Surface Of Mars: New Haven, Yale University Press, 232 p. (6) Greeley, Ronald, and Spudis, P., 1981, Rev. Geophys. Space Phys., 19 pp. 13-41. (7) Cattermole, P., 1987, Jour. Geophys. Res., 92, B4, pp. E553-E560. (8) Pieri, D. C. and Schneeberger, D. M., 1988, Lunar and Planet. Sci. Conf. XIX, pp. 931-932. (9) Mouginis-Mark, P. J., et al., 1988, Bulletin Volcanology, submitted 1987, revised 1988. (10) Schneeberger D. M. and Pieri D. C., 1987, NASA TM-89810, pp. 339-341. (11) Pieri, D. C., et al., 1985, NASA TM-88383, pp. 318-320.

Figure 1. Mosaic showing outlines of major lava flow and volcano-tectonic features at Alba Patera, Mars. Mosaic made from USGS MTM mosaic numbers 35102,-107,-112,-117; 40102, -107,-112,-117; 45102, -107,-112,-117. Scale is 0.9 cm = 50 km.